Thermodynamic assessment of a shipboard BOG reliquefaction system on an LCO_2 carrier based on sea trial data

Viktoriia Sokolovska-Yefymenko[a], Volodymyr Ierin[b], Oleksandr Feshchuk[c], Larisa Morozyuk[a], Oleksandr Yefymenko[a] and Tatiana Morosuk[d]

[a] *Odesa National University of Technology, Ukraine, kli24062006@gmail.com*
[b] *NingboTech University, China, yerinvladimir@gmail.com, CA*
[c] *Babcock Liquid Gas Equipment Limited, United Kingdom, Oleksandr.Feshchuk@babcockinternational.com*
[d] *Technische Universität Berlin, Germany, tetyana.morozyuk@tu-berlin.de*

Abstract:

This paper presents a thermodynamic analysis of a CO_2 boil-off gas (BOG) reliquefaction plant installed on board an LCO_2 carrier, based on sea trial data. The study addresses the emerging field of marine CO_2 transportation, where the number of dedicated vessels remains limited and validated assessments of shipboard system performance are still scarce. Unlike existing studies that rely mainly on steady-state simulations and parametric optimization, this work, for the first time, uncovers the actual structure of thermodynamic irreversibilities under real operating conditions. The analysis is performed using combined energy and exergy models developed from measured process data. The results show that plant efficiency is constrained by localized sources of exergy destruction, despite the high exergy efficiency of most system components, including compressors and key elements of the refrigeration cycle. The dominant source of irreversibility is the throttling of CO_2 upstream of the cargo compressor, which exhibits the highest exergy destruction ratio in the system (app. 21%). This irreversibility is unavoidable and results from the operating constraints imposed by the multi-gas ship design: the suction pressure of the cargo compressor must be reduced to an acceptable level while preventing CO_2 from approaching the triple-point region. A second major source of irreversibility is the heat transfer in the condenser–evaporator. To enhance system performance, it is essential to implement engineering solutions that minimize irreversibilities in pressure control and optimize thermodynamic matching in heat exchangers, while ensuring operational reliability.

Keywords:

CO_2; boil-off gas; reliquefaction plant; LCO_2 carrier; exergy analysis; thermodynamic irreversibility.

1. Introduction

The development of technologies for carbon dioxide capture and geological storage (CCS) drives the need for effective solutions to transport carbon dioxide (CO_2) from emission sources to disposal or injection sites. In areas with limited pipeline infrastructure, sea transportation is viewed as a flexible and cost-effective alternative for certain distances and transport scales [1,2]. At the same time, CO_2 shipping is part of an integrated CCS chain that encompasses liquefaction, storage, transportation, and preparation of CO_2 for storage or injection conditions [2,3]. In recent years, there has been a shift from theoretical solutions to practical applications. Notably, the first specialized ships have been commissioned as part of the Northern Lights project, alongside the development of a new generation of large-capacity LCO_2 carriers [4-6]. This marks the commencement of the operational verification stage for technologies and the development of a new maritime transport segment. Shipboard cargo handling systems are essential for maintaining transportation stability, regulating the CO_2 state within permissible thermodynamic ranges, and controlling the liquid-vapour phase. At the same time, the regulatory framework is largely based on the requirements of the IGC Code, while specialized provisions for the transportation of CO_2 are still in the early stages of development within the IMO [7,8]. The permissible temperature and pressure ranges for CO2 transportation are significantly limited due to the proximity of operating conditions to the triple point [3]. According to [9], two pressure levels of about 7 barg and 15 barg are considered the main ones for marine transportation of CO_2, which correspond to different temperature levels and storage system requirements. A compromise among the liquid CO2 density, the tank design, and the total energy and economic costs determines the choice of mode. Even with effective thermal insulation, heat transfer inevitably leads to the formation of a vapour

phase (boil-off gas, BOG) and an increase in tank pressure [10]. In the case of CO_2, the formation of BOG is directly related to the system exiting the permissible phase range, which requires mandatory treatment of the vapour-gas phase and its return to the liquid state. Thus, reliquefaction systems are integral to ensuring the safe and sustainable operation of CO_2 gas carriers.

Current studies focus on the development and optimization of CO_2-BOG reliquefaction systems. It has been shown that column-flow separation schemes achieve high CO2 recovery but are associated with increased energy intensity and equipment complexity. In contrast, systems with an external refrigeration circuit are better adapted to ship conditions [11]. The configuration choice is determined by the layout limitations, available power, and cooling medium parameters [10].

Exergy analysis of such systems shows that the main losses are concentrated in evaporators, throttling devices, and compressor stages, and that efficiency significantly depends on interstage pressures and heat-exchange parameters [12]. Additional studies demonstrate that impurities affect condensation deterioration and increase energy costs [13,14]. At the same time, it was found that the efficiency of reliquefaction systems is determined not only by the cycle structure, but also by external operational factors, including the cooling medium temperature and the equipment operating modes [15]. A separate area of research focuses on integrating BOG processing systems into the ship's power plant. In particular, the use of cryogenic working media (such as LNG and liquid ammonia) as cooling streams in integrated marine energy and refrigeration systems has been considered [16-18]. Approaches to managing BOG generation are also being developed, including subcooling schemes and accounting for non-condensable chemical components that affect the condensation processes [19,20].

However, the complexity of configurations requires assessment of ship integration, reliability, and operational limitations [21]. The existing research focuses on structural and parametric optimization and relies on stationary models. Such approaches do not reflect the actual conditions of ship operation, characterized by variable loads, changes in cooling medium temperature, and operation of equipment outside design conditions. This leads to a discrepancy between the calculated and actual efficiency of the systems. At the same time, the distribution of irreversibility under actual operating conditions remains insufficiently studied, especially given the system's integration into the ship's power plant.

The purpose of this study is to conduct a thermodynamic assessment of the ship's CO_2-BOG processing system using marine trial data.

2. System description of the CO_2 reliquefaction plant

The CO_2 reliquefaction plant analysed in this study is installed on board a semi-refrigerated LPG/LCO_2 carrier designed for the transportation of liquefied gases at moderate pressures and reduced temperatures. Vessels of this type are widely employed in the marine transport of liquefied petroleum gases and other low-temperature cargoes requiring controlled pressure and temperature conditions during the voyage. The vessel is certified to carry various liquefied gases, including CO_2, ammonia (NH_3), butane (C_4H_0), propane (C_3H_8), propylene (C_3H_6), and vinyl chloride monomer (VCM). The cargo containment system comprises three independent Type C cargo tanks designed as bi-lobe cylindrical pressure vessels for the storage and transportation of liquefied gases at low temperatures. Such an arrangement ensures safe operation under variable thermal and mechanical loads arising during marine transportation and cargo handling operations. The main particulars of the LPG/LCO_2 carrier considered in this study are given in Table 1.

Table 1. *Main characteristics of the LPG/LCO_2 carrier.*

Parameter	Value
Cargo capacity	22,000 m³
Deadweight	27,900 t
Gross tonnage	21,034 GT
Main engine	MAN B&W 6S50ME-C
Specified maximum continuous rating (SMCR)	8,000–9,000 kW
Cargo containment system	Independent Type C pressure tanks
Number of cargo tanks	3

The process flow diagram of the reliquefaction plant operating in the CO_2 carriage mode is shown in Figure 1. The reliquefaction plant is intended for treating BOG generated in cargo tanks due to the heat transfer with the surroundings. Its primary function is to remove CO_2 vapour from the cargo tanks, compress and condense it, and finally return the liquid CO_2 to the cargo system. The plant cargo cycle may be regarded as an open cycle, since the working fluid is removed directly from the cargo containment system and, after

reliquefaction, returned to it. The plant operates on a cascade thermodynamic cycle. The working fluid in the bottoming cascade is CO2, which condenses the cargo vapour. The topping cascade is the refrigeration cycle that operates on propane (R290) and removes heat during CO_2 condensation.

The cargo stage of the cascade includes a three-stage oil-free reciprocating compressor (I) with an intercooling system, the first and second intercoolers (II, III), the LPG condenser (IV), the suction heater (VII), the CO_2 liquid separator (VI), the suction separator (VIII), the pressure control valve $EV1^{CO_2}$, and the expansion valve $EV2^{CO_2}$. The cargo tank (XVI) is connected to the reliquefaction system and serves as the source of the CO_2 (BOG), which is returned to the cargo system after condensation. The refrigerant stage of the cascade includes a single-stage, oil-injected, rotary screw refrigerant compressor (IX), an oil separator (X), a refrigerant condenser (XI), a refrigerant receiver (XII), an oil cooler (XIV), and an oil treatment and filtration unit (XV). The condenser–evaporator (V) provides thermodynamic coupling between the cargo and refrigerant, and serves as the heat-exchange interface between the two circuits. Heat transfer in the intercoolers and the suction heater is provided by a circulating water–glycol mixture. Heat rejection in the LPG condenser and the refrigerant condenser is ensured by seawater cooling.

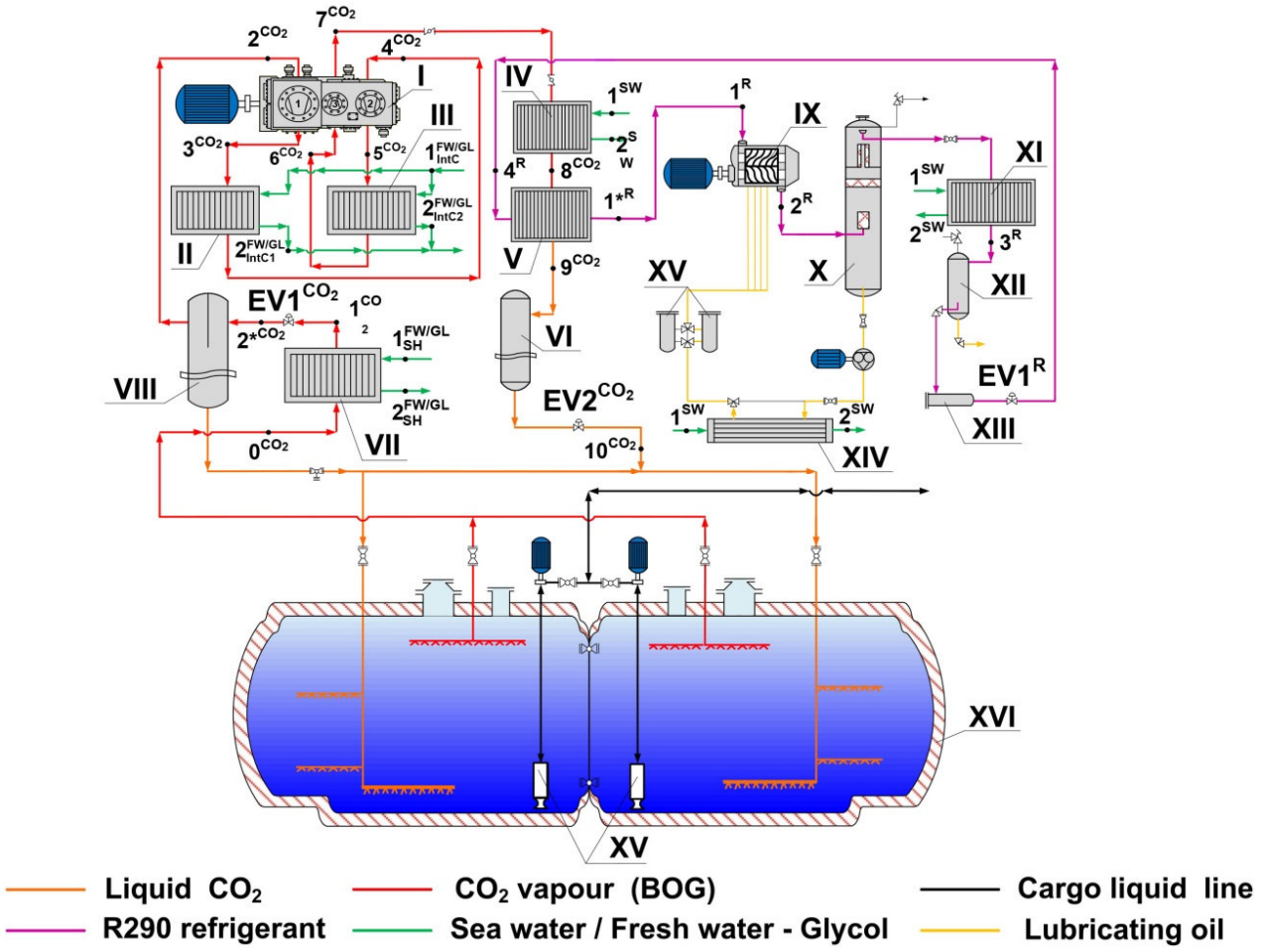

Figure 1. *Schematic diagram of the cascade CO_2 reliquefaction system of the LCO_2 carrier.*

The cargo stage of the cascade operates on a three-stage compression cycle with incomplete intercooling in the intercoolers. A characteristic feature of this cycle is the superheating of the BOG in the suction heater, followed by vapour throttling in the pressure control valve $EV1^{CO_2}$, which ensures stable regulation of the suction pressure at the cargo compressor inlet. The refrigeration stage of the cascade operates according to a conventional single-stage vapour-compression refrigeration cycle using propane (R290) as the refrigerant.

3. Experimental conditions

The experimental data were obtained during the loading operation of liquefied CO_2. At the time of data acquisition, approximately 700 tons of cargo were contained in the cargo tanks. The system was operating under quasi-steady-state conditions, characterized by stable pressure and temperature levels with only minor fluctuations. Process parameters were recorded using the vessel's integrated automation and cargo monitoring system. The analysed dataset comprises cargo tank pressures, the temperature distribution along the tank height, and temperature measurements at the key points of the reliquefaction plant process flow.

The recorded operational data were subjected to preliminary processing, including the selection of a steady operating interval, validation of measurement consistency, and the formation of a set of operating parameters used as input data for the subsequent thermodynamic analysis.

4. Modelling methodology

A thermodynamic model of the CO_2 reliquefaction system was developed based on the experimental data.

The following have been assumed for the model:

- changes in kinetic and potential energy are negligible;
- steady-state operation conditions;
- pressure drops in pipelines and heat exchangers are neglected, as they are small compared to the operating pressures;
- heat exchange with the surroundings is neglected.

The thermodynamic behaviour of the system is evaluated based on the developed energy and exergy models.

4.1. Energy model

The energy model of the CO_2 reliquefaction system was formulated based on the operating parameters of CO_2 and the refrigerant R290 specified at the states the thermodynamic cycle. The thermodynamic properties of CO_2 and R290 were calculated using the NIST REFPROP 10.0, which is based on fundamental equations of state [23]. The thermodynamic cycle of the reliquefaction system is represented in the lgp–h diagrams (Figure 2).

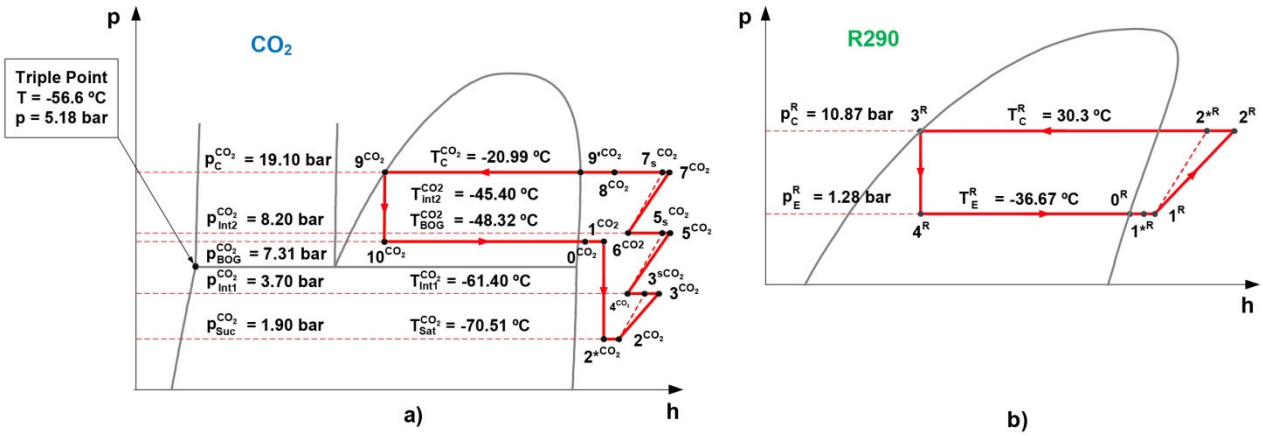

Figure 2. *Thermodynamic cycle of the cascade BOG reliquefaction system in lgp–h diagrams: (a) CO_2 cascade; (b) R290 cascade.*

The energy balances of the reliquefaction system are presented below.

The mass flow rate of CO_2 is determined for the cargo stream at the suction of the first compression stage:

$$\dot{m}_{CO_2} = \frac{\dot{V}_{act,CCI}}{\upsilon_{2^{CO_2}}}, \qquad (1)$$

where $\dot{V}_{act,CCI}$ is the actual volumetric capacity of the compressor; $\upsilon_{2^{CO_2}}$ is the specific volume of CO_2 at the suction of the first compression stage.

The cooling capacity of the reliquefaction system was determined from the energy balance of the cargo stream, which is:

$$\dot{Q}_E = \dot{m}_{CO_2} \cdot \left(h_{liq}^{CO_2} - h_{BOG}^{CO_2} \right), \qquad (2)$$

where $h_{liq}^{CO_2}$ is the specific enthalpy of liquefied CO_2 returned to the cargo tanks; $h_{BOG}^{CO_2}$ is the specific enthalpy of the BOG.

The mass flow rate of the refrigerant R290 was obtained from the energy balance of the condenser–evaporator:

$$\dot{m}_R = \frac{\dot{m}_{CO_2} \cdot \left(h_{in}^{CO_2} - h_{out}^{CO_2}\right)}{h_{out}^{R} - h_{in}^{R}}, \quad (3)$$

where $h_{in}^{CO_2}$ and $h_{out}^{CO_2}$ are the specific enthalpies of CO_2 at the inlet and outlet of the condenser–evaporator (hot side); h_{in}^{R} and h_{out}^{R} are the specific enthalpies of the refrigerant R290 at the inlet and outlet of the condenser–evaporator (cold side).

The heat duty of the k-th heat exchanger is:

$$\dot{Q}_k = \dot{m}_j \cdot \left(h_{in,k}^{j} - h_{out,k}^{j}\right), \quad (4)$$

where $\dot{m}_j$ is the mass flow rate of working stream j, through component k; $h_{in,j}^{k}$ and $h_{out,j}^{k}$ are the specific enthalpies of stream j at the inlet and outlet of component k.

The mass flow rate of the cooling medium (seawater, fresh water, or water-glycol mixture) is:

$$\dot{m}_c = \frac{\dot{Q}_k}{\left(h_{out,k}^{c} - h_{in,k}^{c}\right)}, \quad (5)$$

where *c* denotes the cooling medium.

The power consumption of the cargo compressor stages is:

$$\dot{W}_{CC_i} = \dot{m}_{CO_2} \cdot \left(h_{out,i}^{CO_2} - h_{in,i}^{CO_2}\right), i \in \{I, II, III\}, \quad (6)$$

where index i denotes the compression stage: first (I), second (II), and third (III); $h_{in,i}^{CO_2}$ and $h_{out,i}^{CO_2}$ are the specific enthalpies at the inlet and outlet of the corresponding compression stage.

The total power of the cargo compressor is:

$$\dot{W}_{CC} = \sum_{i=1}^{3} \dot{W}_{CO_2,CC_i}. \quad (7)$$

The power of the refrigerant compressor is:

$$\dot{W}_R = \dot{m}_R \cdot \left(h_{R,out}^{R} - h_{R,in}^{R}\right), \quad (8)$$

where $h_{R,in}^{R}$ and $h_{R,out}^{R}$ are the specific enthalpies at the inlet and outlet of the refrigerant compressor.

The total power consumption of the reliquefaction system is:

$$\dot{W}_{tot} = \dot{W}_{CC} + \dot{W}_R. \quad (9)$$

The isentropic efficiency of the cargo compressor stages is:

$$\eta_{is,CCi} = \frac{h_{out,s,i}^{CO2} - h_{in,i}^{CO2}}{h_{out,i}^{CO2} - h_{in,i}^{CO2}}, \quad (10)$$

where $h_{out,s,i}^{CO_2}$ is the specific enthalpy at the outlet of the i-th stage under isentropic conditions.

The isentropic efficiency of the refrigerant compressor is:

$$\eta_{is,R} = \frac{h_{out,s,i}^{R} - h_{in,i}^{R}}{h_{out,i}^{R} - h_{in,i}^{R}}, \quad (11)$$

where $h_{out,s,i}^{R}$ is the specific enthalpy at the outlet under isentropic conditions.

The specific power consumption of the reliquefaction plant per 1 kg of BOG is:

$$SPC_{BOG} = \frac{\dot{W}_{tot}}{\dot{m}_{CO_2}}. \quad (12)$$

The minimum liquefaction power is:

$$\dot{W}_{min} = \dot{m}_{CO_2} \cdot \left[T_0 \cdot \left(s_{BOG} - s_{liq} \right) - \left(h_{BOG} - h_{liq} \right) \right], \quad (13)$$

where T_0 is the ambient temperature.

The thermodynamic effectiveness of the cascade cycle is:

$$\eta_{th} = \frac{\dot{W}_{min}}{\dot{W}_{tot}}. \quad (14)$$

4.2. Exergy analysis

Exergy analysis is applied to evaluate the performance of the BOG reliquefaction system and to identify sources of irreversibility [23-26].

The total exergy of the k-th material stream consists of physical and chemical components. Since no chemical reactions occur in the system, only the physical exergy is considered:

$$\dot{E}_j^{PH} = \dot{m}_j \cdot e_j^{PH} = \dot{m}_j \cdot \left[\left(h_j - h_0 \right) - T_0 \cdot \left(s_j - s_0 \right) \right], \quad (15)$$

where 0 refers to the values of the substance properties for the same mass flow rate at the reference state (ambient temperature T_0 = 25°C, ambient pressure P_0 = 1.013 bar).

The specific physical exergy is expressed as:

$$e_j^{PH} = e_j^T + e_j^M. \quad (16)$$

The exergy balance for the system and individual components is written as:

$$\dot{E}_{F,tot} = \dot{E}_{P,tot} + \sum_k \dot{E}_{D,k} + \dot{E}_{L,tot}, \quad (17)$$

$$\dot{E}_{F,k} = \dot{E}_{P,k} + \dot{E}_{D,k}, \quad (18)$$

where $\dot{E}_F$, $\dot{E}_P$, $\dot{E}_D$, and $\dot{E}_L$ represent the exergy of fuel, product, destruction, and losses, respectively.

The thermodynamic efficiency ε_{th} and exergy destruction ratio y are:

$$\varepsilon_{th} = \frac{\dot{E}_{P,k}}{\dot{E}_{F,k}} = 1 - \frac{\dot{E}_{D,k} + \dot{E}_{L,k}}{\dot{E}_{F,k}}, \quad (19)$$

$$y_k = \frac{\dot{E}_{D,k}}{\dot{E}_{F,tot}}. \quad (20)$$

The overall exergy efficiency of the BOG reliquefaction system is:

$$\varepsilon_{tot} = \frac{\dot{E}_{P,tot}}{\dot{E}_{F,tot}}. \quad (21)$$

The exergy balance relations used to determine the fuel, product, and exergy destruction for each component of the BOG reliquefaction system are summarized in Table 2.

Table 2. *Equations for exergy analysis of the BOG reliquefaction plant.*

Component	Parameter		
	Exergy of fuel $\dot{E}_{F,k}$	Exergy of product $\dot{E}_{P,k}$	Exergy destruction $\dot{E}_{D,k}$
CO_2 Suction Heater(1)	–	–	$\dot{E}_{D,SH}=\dot{m}_{CO_2}\cdot\left(e^{PH}_{0^{CO_2}}-e^{PH}_{1^{CO_2}}\right)$
CO_2 line superheating	–	–	$\dot{E}_{D,CO_2ls}=\dot{m}_{CO_2}\cdot\left(e^{PH}_{2'^{CO_2}}-e^{PH}_{2^{CO_2}}\right)$
Cargo compressor first stage	$\dot{E}_{F,CCI}=\dot{W}_{CCI}+\dot{m}_{CO_2}\cdot e^{T}_{2^{CO_2}}$	$\dot{E}_{P,CCI}=\dot{m}_{CO_2}\cdot\left(e^{M}_{3^{CO_2}}-e^{M}_{2^{CO_2}}\right)+$ $+\dot{m}_{CO_2}\cdot e^{T}_{3^{CO_2}}$	$\dot{E}_{D,CCI}=\dot{E}_{F,CCI}-\dot{E}_{P,CCI}$
Cargo compressor second stage	$\dot{E}_{F,CCII}=\dot{W}_{CCII}+\dot{m}_{CO_2}\cdot e^{T}_{4^{CO_2}}$	$\dot{E}_{P,CCII}=\dot{m}_{CO_2}\cdot\left(e^{M}_{5^{CO_2}}-e^{M}_{4^{CO_2}}\right)+$ $+\dot{m}_{CO_2}\cdot e^{T}_{5^{CO_2}}$	$\dot{E}_{D,CCII}=\dot{E}_{F,CCII}-\dot{E}_{P,CCII}$
Cargo compressor third stage	$\dot{E}_{F,CCIII}=\dot{W}_{CCIII}+\dot{m}_{CO_2}\cdot e^{T}_{6^{CO_2}}$	$\dot{E}_{P,CCIII}=\dot{m}_{CO_2}\cdot\left(e^{M}_{7^{CO_2}}-e^{M}_{6^{CO_2}}\right)+$ $+\dot{m}_{CO_2}\cdot e^{T}_{7^{CO_2}}$	$\dot{E}_{D,CCIII}=\dot{E}_{F,CCIII}-\dot{E}_{P,CCIII}$
Cargo compressor (in total)	$\dot{E}_{F,CC}=\dot{E}_{F,CCI}+\dot{E}_{F,CCII}+\dot{E}_{F,CCIII}$	$\dot{E}_{P,CC}=\dot{E}_{P,CCI}+\dot{E}_{P,CCII}+\dot{E}_{P,CCIII}$	$\dot{E}_{D,CC}=\dot{E}_{F,CC}-\dot{E}_{P,CC}$
Interstage cooler1 (1)	–	–	$\dot{E}_{D,IC1}=\dot{m}_{CO_2}\cdot\left(e^{PH}_{3^{CO_2}}-e^{PH}_{4^{CO_2}}\right)$
Interstage cooler2 (1)	–	–	$\dot{E}_{D,IC2}=\dot{m}_{CO_2}\cdot\left(e^{PH}_{5^{CO_2}}-e^{PH}_{6^{CO_2}}\right)$
LPG condenser (1)	–	–	$\dot{E}_{D,LPGC}=\dot{m}_{CO_2}\cdot\left(e^{PH}_{7^{CO_2}}-e^{PH}_{8^{CO_2}}\right)$
Condenser–evaporator	$\dot{E}_{F,C\text{-}E}=\dot{m}_{R}\cdot\left(e^{T}_{4^{R}}-e^{T}_{1^{R}}\right)+$ $+\dot{m}_{CO_2}\cdot e^{T}_{8^{CO_2}}$	$\dot{E}_{P,C\text{-}E}=\dot{m}_{CO_2}\cdot e^{T}_{9^{CO_2}}$	$\dot{E}_{D,C\text{-}E}=\dot{E}_{F,C\text{-}E}-\dot{E}_{P,C\text{-}E}$
Expansion valve EV1^{CO2}	$\dot{E}_{F,EV1^{CO_2}}=\dot{m}_{CO_2}\cdot\left(e^{M}_{1^{CO_2}}-e^{M}_{2'^{CO_2}}\right)$	$\dot{E}_{P,EV1^{CO_2}}=\dot{m}_{CO_2}\cdot\left(e^{T}_{2'^{CO_2}}-e^{T}_{1^{CO_2}}\right)$	$\dot{E}_{D,EV1^{CO_2}}=\dot{E}_{F,EV1^{CO_2}}-\dot{E}_{P,EV1^{CO_2}}$
Expansion valve EV2^{CO2}	$\dot{E}_{F,EV2^{CO_2}}=\dot{m}_{CO_2}\cdot\left(e^{M}_{9^{CO_2}}-e^{M}_{10^{CO_2}}\right)+$ $+\dot{m}_{CO_2}\cdot e^{T}_{9^{CO_2}}$	$\dot{E}_{P,EV2^{CO_2}}=\dot{m}_{CO_2}\cdot e^{T}_{10^{CO_2}}$	$\dot{E}_{D,EV2^{CO_2}}=\dot{E}_{F,EV2^{CO_2}}-\dot{E}_{P,EV2^{CO_2}}$
Refrigerant compressor	$\dot{E}_{F,R}=\dot{W}_{R}+\dot{m}_{R}\cdot e^{T}_{1^{R}}$	$\dot{E}_{P,R}=\dot{m}_{R}\cdot e^{T}_{2^{R}}+$ $+\dot{m}_{R}\cdot\left(e^{M}_{2^{R}}-e^{M}_{1^{R}}\right)$	$\dot{E}_{D,R}=\dot{E}_{F,R}-\dot{E}_{P,R}$
Refrigerant condenser (1)	–	–	$\dot{E}_{D,RC}=\dot{m}_{R}\cdot\left(e^{PH}_{2^{R}}-e^{PH}_{3^{R}}\right)$
Expansion valve EV1^{R}	$\dot{E}_{F,EV1^{R}}=\dot{m}_{R}\cdot\left(e^{M}_{3^{R}}-e^{M}_{4^{R}}\right)+$ $+\dot{m}_{R}\cdot e^{T}_{3^{R}}$	$\dot{E}_{P,EV1^{R}}=\dot{m}_{R}\cdot e^{T}_{4^{R}}$	$\dot{E}_{D,EV1^{R}}=\dot{E}_{F,EV1^{R}}-\dot{E}_{P,EV1^{R}}$
Refrigerant line superheating (1)	–	–	$\dot{E}_{D,Rls}=\dot{m}_{R}\cdot\left(e^{PH}_{1'^{R}}-e^{PH}_{1^{R}}\right)$
Overall system	$\dot{E}^{RS}_{F,tot}=\dot{W}_{CC}+\dot{W}_{R}+\dot{m}_{CO_2}\cdot e^{T}_{0^{CO_2}}$	$\dot{E}^{RS}_{P,tot}=\dot{m}_{CO_2}\cdot e^{T}_{10^{E}}$	$\dot{E}^{RS}_{D,tot}=\sum_{k}\dot{E}_{D,k}$

(1) The component is dissipative, for which no exergy of fuel or exergy of product can be defined

5. Results and discussion

The thermodynamic analysis was performed to evaluate the efficiency of the CO_2 reliquefaction plant on an LCO_2 gas carrier under marine trial conditions. The main results of the energy analysis are given in Table 3. The total power consumption of the plant's compressors is $\dot{W}_{tot}$=406.16 kW, of which the three-stage CO_2 cargo compressor accounts for $\dot{W}_{CC}$=206.59 kW, and $\dot{W}_{R}$=199.57 kW is for the screw compressor of the refrigeration stage of the cascade. The isentropic efficiencies of the cargo compressor stages are $\eta_{is,CCI}$=0.659, $\eta_{is,CCII}$=0.819, and $\eta_{is,CCIII}$=0.836. In contrast, for the compressor of the refrigeration stage of the cascade, the value $\eta_{is,R}$=0.771 was obtained. The values obtained correspond to the range characteristic of compressors of the corresponding designs, indicating that the compressor equipment is operating in normal mode during marine trials. The specific energy consumption of the liquefaction process is SPC_{BOG} = 348.33

kJ/kg BOG, and the thermodynamic efficiency of the plant is ηth = 0.270. For cascade reliquefaction plants operating at lower liquefaction temperatures around -100°C, the literature reports thermodynamic efficiencies η_{th} in the range of 0.30-0.45 [27]. This indicates a low thermodynamic efficiency for the system being studied.

An exergy analysis was performed to identify the sources of thermodynamic irreversibilities. The distribution of exergy efficiency ε_k across the main productive components of the BOG reliquefaction system is shown in Figure 3. The components are ranked by ε_k and grouped into three zones: Poor, Acceptable, and Excellent.

As can be seen in Figure 3, most components are located in the Acceptable and Excellent zones based on the exergy efficiency of the components ε_k. These include the second and third stages of the cargo compressor with ε_k=85.19% and 86.86%, the cargo compressor as a whole — 80.87%, the refrigerant compressor — 80.81%, as well as the expansion valve $EV2^{CO_2}$: 94.8 %. The first stage of the cargo compressor is characterized by a reduced ε_k value of 70.09 %, but remains above the conditional limit for unsatisfactory operation. The minimum exergy efficiency values are observed for the pressure regulator $EV1^{CO_2}$ (pressure control valve) ε_k=0.39% and the cascade heat exchanger (condenser–evaporator) ε_k=65.55%, indicating their decisive influence on the overall thermodynamic efficiency of the reliquefaction plant.

Table 3. *Energy analysis results of the BOG reliquefaction plant.*

Parameter	Value
Cooling capacity $\dot{Q}_E$, kW	340.32
CO_2 mass flow rate in the cargo cascade $\dot{m}_{CO2}$, kg/s	1.166
Propane mass flow rate in the refrigerant cascade $\dot{m}_R$, kg/s^{-1}	1.416
Mass flow rate of FW/GL through the CO_2 suction heater $\dot{m}_{FW/GL,SH}$, kg/s	3.962
Mass flow rate of FW/GL through the interstage cooler 1 $\dot{m}_{FW/GL,IC1}$, kg/s	3.710
Mass flow rate of FW/GL through the interstage cooler 2 $\dot{m}_{FW/GL,IC2}$, kg/s	4.190
Fresh water mass flow rate through the LPG condenser $\dot{m}_{SW/LPGC}$, kg/s	3.140
Fresh water mass flow rate through the refrigerant condenser $\dot{m}_{SW/RC}$, kg/s	20.254
Heat load of the CO_2 suction heater $\dot{Q}_{SH}$, kW	52.34
Heat load of the interstage cooler 1 $\dot{Q}_{IC1}$, kW	49.15
Heat load of the interstage cooler 2 $\dot{Q}_{IC2}$, kW	69.55
Heat load of the LPG condenser $\dot{Q}_{LPGC}$, kW	92.00
Heat load of the refrigerant condenser $\dot{Q}_R$, kW	593.06
Isentropic efficiency of the compressor first stage $\eta_{is,CCI}$	0.659
Isentropic efficiency of the compressor second stage $\eta_{is,CCII}$	0.819
Isentropic efficiency of the compressor third stage $\eta_{is,CCIII}$	0.836
Isentropic efficiency of the refrigerant compressor $\eta_{is,R}$	0.771
Power consumption of the compressor first stage $\dot{W}_{CCI}$, kW	66.52
Power consumption of the compressor second stage $\dot{W}_{CCII}$, kW	68.75
Power consumption of the compressor third stage $\dot{W}_{CCIII}$, kW	71.32
Total power consumption of the cargo compressor $\dot{W}_{CC}$, kW	206.59
Power consumption of the refrigerant compressor $\dot{W}_R$, kW	199.57
Total power consumption of the cascade cycle $\dot{W}_{tot}$, kW	406.16
Specific power consumption of the reliquefaction plant SPC_{BOG}, kJ/kg$_{BOG}$	348.33
Minimum liquefaction power $\dot{W}_{min}$, kW	110.50
Thermodynamic effectiveness of the reliquefaction plant η_{th}	0.270

The distribution of the exergy destruction ratio y_k (Figure 4) confirms this conclusion. The largest part of exergy destruction is accounted for by the pressure control valve $EV1^{CO_2}$, where y_k=20.86% of the total destruction of the system. A significant contribution is made by the refrigerant compressor (9.64%), the cargo compressor as a whole (9.54%), and the condenser–evaporator (8.36%). For individual stages of the cargo compressor, the y_k values are 4.84%, 2.46%, and 2.27%, respectively. The remaining components of the system form a significantly smaller proportion of the total y_k. Thus, the main sources of thermodynamic irreversibility are: process pressure reduction before the cargo compressor and interstage heat exchange.

The increased exergy destruction ratio yk and the relatively low exergy efficiency of the cascade heat exchanger are due to its operation at significant temperature and pressure differences between the two stages. According to marine trial data, the calculated logarithmic mean temperature difference (LMTD) for this heat exchanger is about 28.1°C, while the design documentation indicates a corrected LMTD of 8.8°C. Thus, the actual temperature and pressure exceed the calculated values by 3.2 times, indicating a significant temperature mismatch between the flows and leading to an increase in exergy destruction in this component.

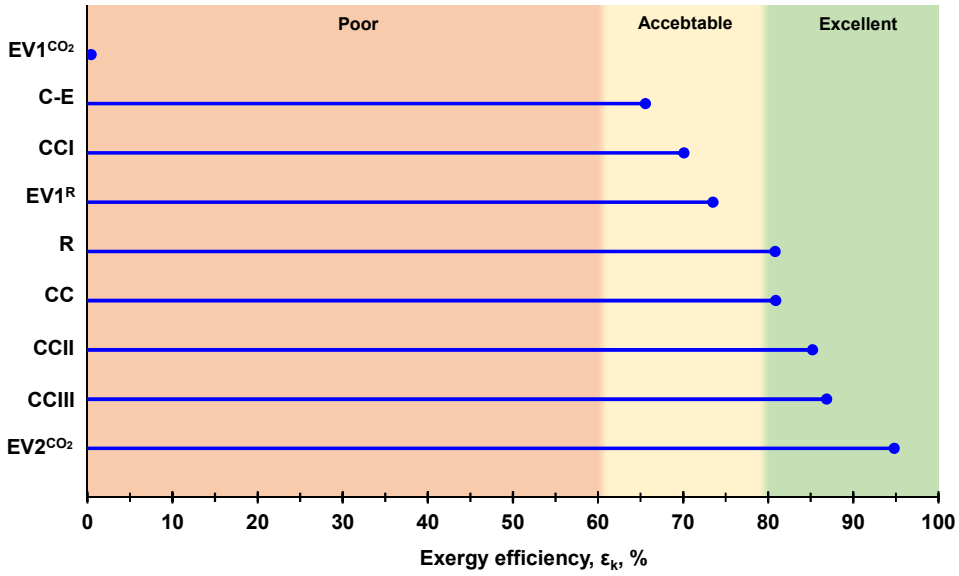

Figure 3. *Exergy efficiency of the productive components of the BOG reliquefaction plant.*

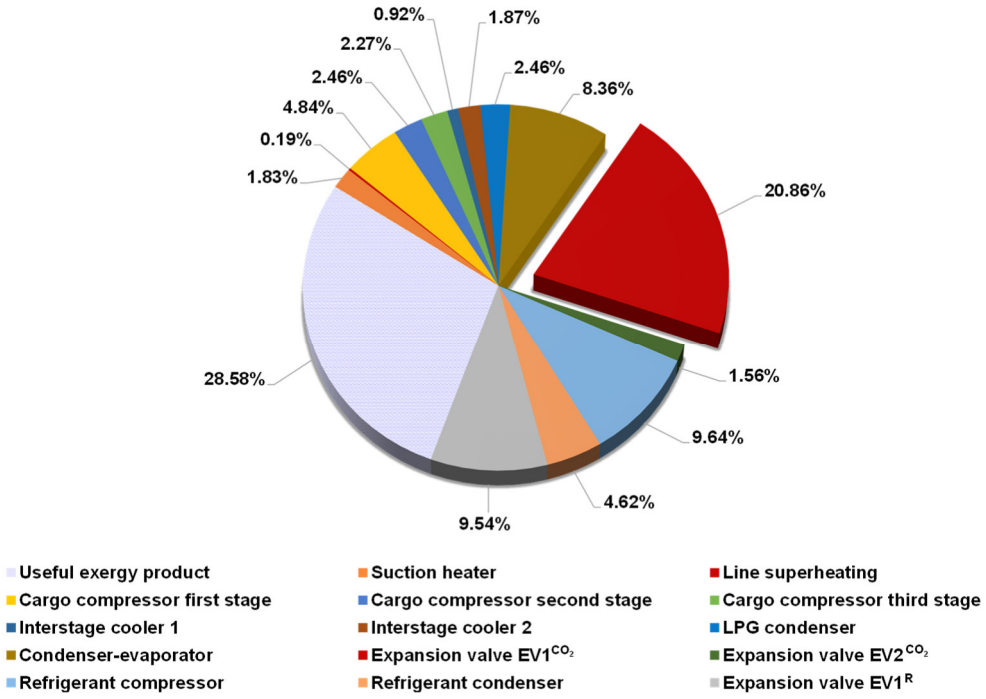

Figure 4. *Distribution of the exergy destruction ratio* y_k *among the components of the BOG reliquefaction plant.*

The dominant source of thermodynamic irreversibility is the pressure control valve $EV1^{CO_2}$. The minimum value of exergy efficiency ε_k and the maximum value of exergy destruction ratio y_k for this component show that the process of reducing the vapor pressure of the CO_2 phase in front of the compressor is the most thermodynamically unfavourable in the presented system. Unlike in classic expansion valves, where two-phase flow is formed, superheated steam is throttled in the EV1CO2, leading to additional irreversibility.

At the same time, this pressure control method is used due to design limitations in the ship's system. The vessel is a universal gas carrier designed to transport various liquefied gases, which determines the pressure range of the cargo compressor. When transporting CO_2, the pressure in the cargo tanks reaches about 6 barg, exceeding the compressor's allowable suction pressure. Under these conditions, a preliminary pressure reduction is required. Reducing the storage pressure of CO_2 to atmospheric levels should not be considered due to the risk of transition to the triple point of co_2 and the formation of a solid phase. Consequently, throttling in the pressure control valve $EV1^{CO_2}$ constitutes a forced operational compromise given the versatility of the ship's cargo system and the thermodynamic properties of CO_2.

To visually represent the distribution of exergetic flows in the system, Figure 5 shows the Grassmann diagram of exergy flows. It follows from the diagram that the total fuel exergy supplied to the system is about $\dot{E}_{F,tot} \approx 414$ kW, while product exergy $\dot{E}_{P,tot}$ is about 118 kW. The rest of the supplied exergy is converted to exergy destruction: $\dot{E}_{D,tot} \approx 296$ kW.

Taking into account the revealed distribution of irreversibilities, the potential directions for increasing the reliquefaction plant's efficiency primarily involve improving interstage heat exchange and the pressure-reduction process upstream of the compressor. An increase in the efficiency of the interstage heat exchanger can be achieved by matching the mass flow rates and improving the temperature matching of the flows. For the expansion valve $EV1^{CO_2}$, a theoretically feasible improvement direction is the use of partial-pressure-drop recovery devices (for turboexpanders or ejector-based systems). However, the use of turboexpanders in such marine systems is limited by the lack of commercially available solutions designed for CO_2 operating modes. The use of ejector-based systems, in turn, may be accompanied by operational stability problems under variable load and dynamic marine operating conditions. Thus, further research should focus on developing compromise engineering solutions that reduce the irreversibility of the pressure-reduction process while maintaining the structural simplicity and operational reliability of the BOG reliquefaction system. A particular difficulty of this task is the universal nature of the gas carrier's cargo system, which requires efficient operation of the reliquefaction plant across a range of thermodynamic cargo conditions.

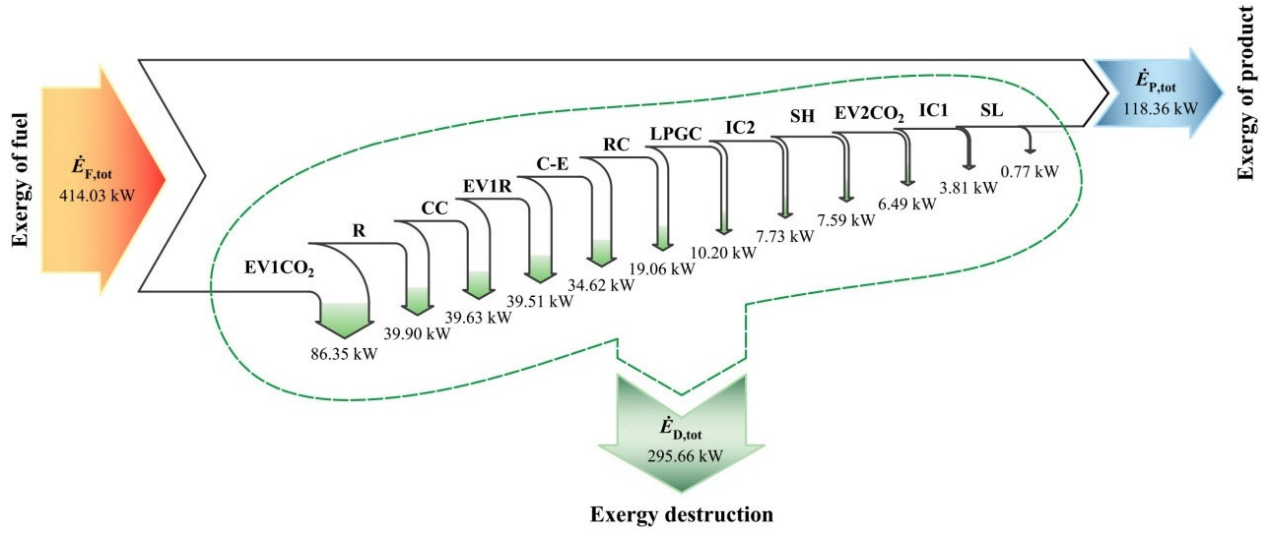

Figure 5. *Grassmann diagram of exergy flows and exergy destruction in the BOG reliquefaction system.*

6. Conclusions

The paper presents, for the first time, a thermodynamic analysis of a CO_2-BOG reliquefaction plant installed on board an operating LCO_2 carrier, based on sea-trial data. The use of measured operational parameters enabled the system's energy and exergy efficiencies to be quantified during actual ship operation and the identification of the components that form the structure of thermodynamic irreversibilities.

The energy analysis showed that the reliquefaction plant's cooling capacity is 340 kW, the total compressor power consumption is 406 kW, and the specific energy consumption of the liquefaction process is 348 kJ/kg_{BOG}. The isentropic efficiency of the compressors is 0.66–0.84, which aligns with the performance characteristics of this type of compressor equipment and confirms the system's stable operation in sea-trial mode.

Exergy analysis showed that the total fuel exergy of the system is 414 kW, product exergy — 118 kW, and total exergy destruction — 296 kW, corresponding to a thermodynamic efficiency of 0.27. The values obtained reflect the influence of irreversible processes characteristic of marine reliquefaction systems, in which a significant part of the supplied exergy is destroyed during heat exchange and pressure regulation.

At the same time, most of the plant's productive components exhibit high exergy efficiency, including compressors and the main components of the refrigeration circuit. The exergy efficiency values of the cargo compressor reach 80.9%, the refrigerant compressor — 80.8%, and the individual components of the refrigeration circuit exceed 90%, confirming the high thermodynamic efficiency of a significant part of the equipment.

The greatest contribution to the structure of exergetic irreversibilities is made by the pressure control valve $EV1^{CO_2}$ and the interstage heat exchanger (condenser–evaporator). For $EV1^{CO_2}$, exergy efficiencies of 0.39% and exergy destruction ratios of 20.86% were obtained, due to throttling of superheated CO2 vapor before

the compressor and the complete loss of potential expansion work. For a condenser–evaporator, the exergy efficiency is 65.55%, and the exergy destruction ratio is 8.36%, due to the operation of the device at a temperature and pressure exceeding the design value.

The results show that the main limitation of the plant's efficiency is related to the irreversibility of the processes of lowering the CO_2 pressure in front of the compressor and condenser–evaporator. For ships of the LCO_2 carrier type, efficiency improvements should be considered while accounting for operational reliability, equipment stability, and the versatility of the cargo system.

The study shows that using sea-trial data enables the identification of the real sources of thermodynamic irreversibilities in marine CO_2 reliquefaction plants. The results obtained can be used in the design and optimization of BOG processing systems on ships of the LCO_2 carrier type, as well as in the development of energy-efficient technologies for the marine transportation of liquefied CO_2.

Nomenclature

e specific exergy, kJ/kg
Ė exergy, kW
h enthalpy, kJ/kg
ṁ mass flow rate, kg/s
P pressure, bar or barg
Q̇ heat load, kW
T temperature, K or °C
Ẇ power consumption, kW
y exergy destruction ratio, %

Greek symbols

η efficiency
ε exergy efficiency

Subscripts and superscripts

CC cargo compressor
D destruction
E evaporator
F fuel
in inlet
k component
out outlet
P product
R refrigerant compressor, refrigerant
th thermodynamic
tot total

References

[1] Kjärstad J., Skagestad R., Eldrup N.H., Johnsson F., Ship transport – A low cost and low risk CO_2 transport option in the Nordic countries. Int J Greenh Gas Control 2016;54:168-84.

[2] Al Baroudi H., Awoyomi A., Patchigolla K., Jonnalagadda K., Anthony E.J., A review of large-scale CO_2 shipping and marine emissions management for carbon capture, utilisation and storage. Appl Energy 2021;287:116510.

[3] Seo Y., Huh C., Lee S., Chang D., Comparison of CO_2 liquefaction pressures for ship-based carbon capture and storage (CCS) chain. Int J Greenh Gas Control 2016;52:1-12.

[4] Northern Lights JV. Northern Lights' first CO_2 transport ship ready for delivery. 2024. – Available at:<https://norlights.com/news/northern-lights-first-co2-transport-ship-ready-for-delivery/> [accessed 25.3.2026].

[5] Kawasaki Kisen Kaisha, Ltd. Delivery of liquefied CO_2 carrier "Northern Phoenix". 2025. – Available at:<https://www.kline.co.jp/en/news/liquefied_gas/liquefied_gas-20251203.html> [accessed 25.3.2026].

[6] Capital Clean Energy Carriers. LCO_2 carrier ACTIVE – Completion of Gas Trials. Press release, 18 Dec 2025. – Available at:<https://www.capitalcleanenergycarriers.com/news-releases/news-release-details/lco2-carrier-active-completion-gas-trials> [accessed 25.3.2026].

[7] IMO Resolution. MSC.370(93). 2014 Amendments to the International Code for the Construction and Equipment of Ships Carrying Liquefied Gases in Bulk (IGC Code). 2014 – Available at:<https://wwwcdn.imo.org/localresources/en/KnowledgeCentre/IndexofIMOResolutions/MSCResolutions/MSC.370(93).pdf> [accessed 25.3.2026].

[8] IMO. CCC 10/16. 2024 Report to the Maritime Safety Committee and the Marine Environment Protection Committee. 2024. Available at:< https://assets.eu.ctfassets.net/jchk06tdml2i/CA6B5EHhmZ7j11TztFYDF/9c5e16da60951f7746ddaecd4f7937d5/CCC_10-16_Report_to_the_MSC_and_MEPC_31_Oct_2024.pdf> [accessed 17 May 2025].

[9] Roussanaly S., Deng H., Skaugen G., Gundersen T., At what Pressure Shall CO_2 Be Transported by Ship? An in-Depth Cost Comparison of 7 and 15 Barg Shipping. Energies 2021;14(18):5635.

[10] Jeon S.H., Choi Y.U., Kim M.S., Review on Boil-Off Gas (BOG) Reliquefaction System of Liquefied CO_2 Transport Ship for Carbon Capture and Sequestration (CCS). Int J Air-Cond Refrig 2016;24(03):1650017.

[11] Lee Y., Baek K.H., Lee S., Cha K., Han C., Design of boil-off CO_2 reliquefaction processes for a large-scale liquid CO_2 transport ship. Int J Greenh Gas Control 2017;67:93-102.

[12] Ketfi M., Ouadha A., Exergy analysis of a CO_2 boil-off gas reliquefaction system. Int J Energy Clean Environ 2021;22(2):1-16.

[13] Jeon S.H., Kim M.S., Compressor selection methods for multi-stage reliquefaction system of liquefied CO_2 transport ship for CCS. Appl Therm Eng 2015;82:360-7.

[14] Jeon S.H., Kim M.S., Effects of impurities on the reliquefaction system of liquefied CO_2 transport ship for CCS. Int J Greenh Gas Control 2015;43:225-32.

[15] Yoo B-Y., The development and comparison of CO_2 BOG reliquefaction processes for LNG fueled CO_2 carriers. Energy 2017;127:186-97.

[16] Lee S.G., Choi G.B., Lee C.J., Lee J.M., Optimal design and operating condition of boil-off CO_2 reliquefaction process, considering seawater temperature variation and compressor discharge temperature limit. Chem Eng Res Design 2017;124:29-45.

[17] Lu J., Li Y., Li B., Yang Q., Deng F., Research on reliquefaction of cargo BOG using liquid ammonia cold energy on CO_2 transport ship. Int J Greenh Gas Control 2023;129:103994.

[18] Kim J.-S., Kim D.-Y., Thermodynamic and Economic Analysis of Cargo Boil-Off Gas Reliquefaction Systems for Ammonia-Fueled LCO_2 Carriers. J Mar Sci Eng 2024;12(9):1642.

[19] Lee J., Son H., Oh J., Yu T., Kim H., Lim Y., Advanced process design of subcooling reliquefaction system considering storage pressure for a liquefied CO_2 carrier. Energy 2024;293:130556.

[20] Jeong I., Jeon Y., Shin H., Lee J., Lim Y., Optimization and economic evaluation of carbon dioxide BOG reliquefaction process considering storage pressure and nitrogen impurity. Energy 2025;323:135837.

[21] Noh H., Kang K., Techno-economic analysis of large-scale CO_2 ship transport with onboard boil-off gas reliquefaction. Int J Greenh Gas Control 2025;142:104337.

[22] Lemmon E.W., Bell I.H., Huber M.L., McLinden M.O., Reference fluid thermodynamic and transport properties database (REFPROP). 10.0 ed. Gaithersburg, Maryland, USA: National Institute of Standards and Technology, NIST Standard Reference Database 23; 2018.

[23] Tsatsaronis G., Winhold M., Exergoeconomic analysis and evaluation of energy-conversion plants — I. A new general methodology. Energy 1985;10(1):69-80.

[24] Tsatsaronis G., Definitions and nomenclature in exergy analysis and exergoeconomics. Energy 2007;32(4):249-53.

[25] Morosuk T., Tsatsaronis G., Advanced exergetic evaluation of refrigeration machines using different working fluids. Energy 2009;34(12):2248-58.

[26] Morosuk T., Tesch S., Hiemann A., Tsatsaronis G., Bin Omar N., Evaluation of the PRICO liquefaction process using exergy-based methods. J Nat Gas Sci Eng 2015;27:23-31.

[27] Sokolovska-Yefymenko V., Morozyuk L., Ierin V., Khliyeva O., Feshchuk O., Yefymenko O., Evaluation of the ethane reliquefaction system integrated with the fuel gas supply system of the large ethane carrier. Energy 2025;330:136884.